Spectrochimica Acta Part A: Molecular and Biomolecular Spectroscopy 130 (2014) 198–207

Contents lists available at ScienceDirect

Spectrochimica Acta Part A: Molecular and Biomolecular Spectroscopy

journal homepage: www.elsevier.com/locate/saa

Experimental and computational study on 2,2′-[(1E,2E)-hydrazine-1,2-diylidenedi(1E)eth-1-yl-1-ylidene]diphenol and its Ni(II), Pt(II), Pd(II) complexes

Saliha Alyar [a,*], Neslihan Özbek [b], Sema Öztürk Yıldırım [c,d], Semra İde [e], Ray J. Butcher [c]

[a] Department of Chemistry, Science Faculty, Karatekin University, TR-18100 Çankırı, Turkey
[b] Department of Primary Education, Faculty of Education, Ahi Evran University, 40100 Kırşehir, Turkey
[c] College of Arts & Sciences, Department of Chemistry, Howard University, 525 College Street NW, Washington, DC 20059, USA
[d] Department of Physics, Faculty of Sciences, Erciyes University, 38039 Kayseri, Turkey
[e] Department of Physics Engineering, Faculty of Engineering, Hacettepe University, 06800 Beytepe, Ankara, Turkey

HIGHLIGHTS

- 2,2′-[(1E,2E)-hydrazine-1,2-diylidenedi(1E)eth-1-yl-1-ylidene]diphenol (L).
- $[Ni_2L_2]$, $[Pt_2L_2]$ and $[Pd_2L_2]$ characterization of compounds.
- ^1H and ^{13}C shielding tensors for crystal structure with GIAO/DFT/B3LYP/6-311++G(d,p) methods.
- The vibrational band assignments for crystal structure with B3LYP/6-311++G(d,p)/(SQMFF).
- Antimicrobial activities of compounds.

GRAPHICAL ABSTRACT

2,2′-[(1E,2E)-hydrazine-1,2-diylidenedi(1E)eth-1-yl-1-ylidene]diphenol and its dimeric, binuclear Ni(II), Pd(II) and Pt(II) metal complexes were synthesized and investigated their antibacterial activities.

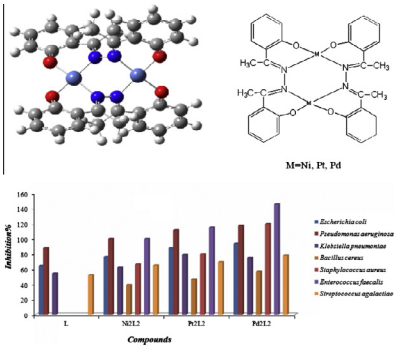

ARTICLE INFO

Article history:
Received 3 February 2014
Received in revised form 5 March 2014
Accepted 18 March 2014
Available online 12 April 2014

Keywords:
Hydrazine
Complex
Antibacterial activity
X-ray
HOMO
LUMO

ABSTRACT

2,2′-[(1E,2E)-hydrazine-1,2-diylidenedi(1E)eth-1-yl-1-ylidene]diphenol and its dimeric, binuclear Ni(II), Pd(II) and Pt(II) metal complexes were synthesized. Hydrazine derivative and its complexes were characterized by elemental analyses, LC-MS, IR, electronic spectra, ^1H and ^{13}C NMR spectra, conductivity and magnetic measurements. ^1H and ^{13}C shielding tensors for crystal structure were calculated with GIAO/DFT/B3LYP/6-311++G(d,p) methods in $CDCl_3$. The vibrational band assignments were performed at B3LYP/6-311++G(d,p) theory level combined with scaled quantum mechanics force field (SQMFF) methodology. The antibacterial activities of synthesized compounds were studied against some Gram-positive and Gram-negative bacteria by using the microdilution and disk diffusion method. As the antibacterial activity results evidently show, the compound possessed a broad spectrum of activity against the tested bacteria.

* Corresponding author. Tel.: +90 376 218 1123; fax: +90 376 218 1031.
E-mail address: saliha@karatekin.edu.tr (S. Alyar).

http://dx.doi.org/10.1016/j.saa.2014.03.034
1386-1425/

Introduction

Compounds containing azomethine group (—C=N—) in the structure are known as hydrazine [1], which are usually synthesized by the condensation of primary amines and active carbonyl groups. Hydrazine is widely used as a raw material in the manufacture of agricultural chemicals, a powerful reducing agent in fuel cells [2], plant growth regulators, polymerizations catalysts, intermediates in industrial preparations of pesticides, corrosion inhibitor and antioxidant [3]. It is also very important in pharmacology, because it is recognized as a carcinogenic, hepatotoxic and mutagenic substance [4,5]. It has been reported that hydrazine and its derivatives have adverse health effects [6]. Therefore, sensitive detections of hydrazine are practically important for environmental and biological analysis [7–12]. The chemistry of hydrazine complexes of transition metals has developed extensively in recent years [13,14], mainly due to their close relationship with the dinitrogen fixation process [15,16]. Many hydrazine complexes have thus been synthesized and several reactivity studies have been reported [13,14].

We present the results of a detailed investigation of the synthesis and structural characterization of 2′-[(1E,2E)-hydrazine-1,2-diylidenedi(1E)eth-1-yl-1-ylidene]diphenol and its Ni(II), Pd(II) and Pt(II) metal complexes using elemental analyses, LC-MS, FT-IR, NMR and quantum chemical methods. ^{1}H and ^{13}C NMR chemical shifts of the ligand compound in the ground state have been calculated by using the GIAO/DFT/B3LYP methods with 6-311++G(d,p) basis set. The vibrational band assignments were performed at B3LYP/6-311++G(d,p) theory level combined with scaled quantum mechanics force field (SQMFF) methodology The vibrational frequencies, ^{13}C and ^{1}H NMR chemical shifts values for the mentioned compound are consistent with the experimental data. Furthermore, the highest occupied molecular orbital (HOMO) and the lowest unoccupied molecular orbital (LUMO) have been simulated, all synthesized compounds have been determined using ab initio calculations. Additionally, the title compound was tested for in vitro antibacterial activity against five Gram-positive bacteria (*Bacillus subtilis* ATCC 6633, *Bacillus cereus* NRRL-B-3711, *Staphylococcus aureus* ATCC 6538, *Enterococcus faecalis* ATCC 29212, *Streptococcus agalactiae* ATCC 13813 and three Gram-negative bacteria (*Escherichia coli* ATCC 11230, *Pseudomonas aeruginosa* ATCC 15442, *Klebsiella pneumoniae* ATCC 70063) by both disc diffusion and microdilution methods.

Experimental

Instrumentation

The elemental analysis (C, H, N and S) were performed on a LECO–CHSNO – 9320 type elemental analyzer. The IR spectra (4000∼400 cm^{-1}) were recorded on a Mattson-1000 FT-IR spectrophotometer with samples prepared as KBr pellets. NMR spectra were recorded on a Bruker Spectrospin Avance DPX-400 Ultra – Shield (400 MHz) Spectrometer by using $CDCl_3$ as a solvent and TMS as an internal standard. LC/MS-APCl was recorded on AGILENT 1100. The melting point was recorded on OptiMelt apparatus. TLC was conducted on 0.25 mm silica gel plates (60F254, Merck). The molar magnetic susceptibilities were measured on powdered samples using Gouy method. The molar conductance measurements were carried out using a Siemens WPA CM 35 conductometer. All solvents purchased from Merck and reagents were obtained from Aldrich Chem. Co. (ACS grade) and used as received. The experiments were carried out in a dynamic nitrogen atmosphere (20 mL/min) with a heating rate of 10 °C/min in the temperature range 30∼400 °C using platinum crucibles.

Synthesis of 2′-[(1E,2E)-hydrazine-1,2-diylidenedi(1E)eth-1-yl-1-ylidene]diphenol

Acetophenone (0.01 mol, 1.34 g) in ethanol (20 mL) and hydrazine monohydrate (0.01 mol, 0.5 g) in ethanol was refluxed on a water bath for 10 h. The progress of reaction was monitored by TLC at appropriate time intervals. The solution was poured onto crushed ice and kept aside. The precipitate thus separated was collected by filtration, suspended in water and neutralized with $NaHCO_3/K_2CO_3$ to give the desired product. The product was recrystallized from chloroform [17]. Yield 85%; mp: 448 K. EI-MS (70 eV) *m*/*z*: 264.8, (M^+, 10.5%, M^{+1}, 18.9%); Elemental analysis: Calcd for $C_{16}H_{16}N_2O_2$: C, 81.78; H, 7.63; N, 10.60. Found: C, 81.54; H, 7.79; N, 10.45.

Synthesis of Ni(II), Pt(II), Pd(II) complexes

All complexes are prepared by the following general method: a sample of anhydrous 0.80 mmol MCl_2, where M: Ni(II) [18], Pt(II) and Pd(II) were dissolved in a mixture of methanol and acetonitrile (2/1, 30 mL) and a solution of hydrazine (2.0 mmol) in a mixture of acetonitrile (2.0 mL) and NaOH solution in methanol (2.0 mL) was added. The reaction mixture was heated at 60 °C for 1 h. The complexes precipitated guickly after stirring the mixture at room temperature and filtered off, dried in a desiccator over $CaCl_2$.

[Ni_2L_2] ($C_{32}H_{28}N_4O_4Ni_2$): Yield 70%; mp: 287–289 °C. EI-MS (70 eV) *m*/*z*: 648.08, (M^+, 100.0%), M^{+2}, 38.5%); Elemental analysis: Calcd for C, 59.13; H, 4.34; N, 8.62; Ni, 18.06. Found: C, 59.16; H, 4.35; N, 8.54; Ni, 18.85.

[Pt_2L_2] ($C_{32}H_{28}N_4O_4Pt_2$): Yield 70%; mp: 320–322 °C. EI-MS (70 eV) *m*/*z*: 922.75, (M^+, 100%, M^{+1}, 83.2%); Elemental analysis: Calcd for C, 41.65; H, 3.06; N, 6.07; Pt, 42.28. Found: C, 41.16; H, 3.08; N, 6.04; Pt, 42.30.

[Pd_2L_2] ($C_{32}H_{28}N_4O_4Pd_2$)Yield 80%; mp: 294–296 °C. EI-MS (70 eV) *m*/*z*: 744.02, (M^+, 100%, M^{+1}, 376.03%); Elemental analysis: Calcd for C, 51.56; H, 3.79; N, 7.52; Pd, 28.55. Found: C, 51.11; H, 3.75; N, 7.22; Pd, 28.05.

Crystallographic studies

Suitable single crystal of size 0.50 × 0.40 × 0.40 mm was selected for X-ray diffraction. The intensity data were collected at room temperature on an Oxford Diffraction Xcalibur Ruby Gemini diffractometer using graphite-monochromated Mo Kα radiation (λ = 0.7107 Å). Data were corrected for Lorenz and polarization effects, and an absorption correction was made using the multi-scan method [19]. The intensity data were collected by ω scan mode within $3.2° \leqslant \theta \leqslant 28.5°$ for $-8 \leqslant h \leqslant 6$, $-13 \leqslant k \leqslant 18$, $-15 \leqslant l \leqslant 21$ in the orthorhombic crystal system. The structures were solved by direct methods using *SHELXS97* and refined by full-matrix least squares *SHELXL97* [20]. All non-hydrogen atoms were refined anisotropically. Final refinement on F^2 by full-matrix least squares method was performed on positional parameters of all atoms, anisotropic vibrational parameters of all non-H-atoms and isotropic temperature factors of hydrogen atoms. Non-hydrogen atoms were located by direct methods. All H atoms were positioned geometrically and allowed to ride on their parent atoms, with d(C—H) = 0.93 Å for aromatic and 0.96 Å for CH_3 atoms. The U_{iso} values were constrained to be 1.5 U_{eq} of the carrier atom for methyl H atoms and 1.2 U_{eq} for the remaining H atoms. A rotating group model was used for the methyl groups. Weighting scheme was used in the form: $w = 1/[\sigma^2(F_o^2) + (0.0728P)^2 + 0.0195P]$ where $P = (F_o^2 + 2F_c^2)/3$. Crystal data and structure refinement details are presented in Table 1.

Table 1
Crystal data and refinement details for 2,2′-[(1E,2E)-hydrazine-1,2-diylidenedi(1E)eth-1-yl-1-ylidene]diphenol.

$C_{16}H_{16}N_2O_2$	D_x = 1.289 Mg m^{-3}
M_r = 268.31	Mo Kα radiation, λ = 0.71073 Å
Orthorhombic, *P2ac2ab*	Cell parameters from 1933 reflections
a = 6.3533 (5) Å	θ = 3.2–28.5°
b = 13.5769 (10) Å	μ = 0.09 mm^{-1}
c = 16.0298 (10) Å	T = 123 K
V = 1382.69 (17) Å^3	Block, yellow
Z = 4	0.50 × 0.40 × 0.40 mm
F(000) = 568	2134 reflections with $I > 2\sigma(I)$
Xcalibur, Ruby, Gemini diffractometer	R_{int} = 0.035
Radiation source: Enhance (Mo) X-ray source	θ_{max} = 28.6°, θ_{min} = 3.3°
Graphite	h = −8.6
Detector resolution: 10.5081 pixels mm^{-1}	k = −13.18
ω Scans	l = −15.21
4438 Measured reflections	Hydrogen site location: inferred from neighboring sites
2718 Independent reflections	H-atom parameters constrained
Refinement on F^2	$w = 1/[\sigma^2(F_o^2) + (0.0728P)^2 + 0.0195P]$ where $P = (F_o^2 + 2F_c^2)/3$
Least-squares matrix: full	$(\Delta/\sigma)_{max}$ = 0.002
$R[F^2 > 2\sigma(F^2)]$ = 0.046	$\Delta\rho_{max}$ = 0.17 e Å^{-3}
$wR(F^2)$ = 0.130	$\Delta\rho_{min}$ = −0.12 e Å^{-3}
S = 1.04	Flack parameter: −1.7 (16)
2718 Reflections	187 Parameters

Absolute structure: H.D. Flack, Acta Cryst. A39 (1983) 876–881.
Primary atom site location: structure-invariant direct methods.
Secondary atom site location: difference Fourier map.

Antimicrobial activity

B. subtilis ATCC 6633, *B. cereus* NRRL-B-3711, *S. aureus* ATCC 6538, *E. faecalis* ATCC 29212, *S. agalactiae* ATCC 13813, *Escherichia coli* ATCC 11230, *P. aeruginosa* ATCC 15442, *K. pneumoniae* ATCC 70063 cultures were obtained from Gazi University, Biology Department and Hacettepe University, Biology Department and bacterial strains were cultured overnight at 310 K in a nutrient broth. During the survey, these stock cultures were stored in the dark at 277 K.

The synthesized compounds were dissolved in dimethylsulfoxide (20% DMSO) to a final concentration of 6.0 mg mL^{-1} and sterilized by filtration with 0.45 μm Millipore filters. Antimicrobial tests were then carried out by the disc diffusion method using 100 μL of suspension containing 10^8 CFU mL^{-1} bacteria spread on a nutrient agar (NA) medium. The discs (6 mm in diameter) were impregnated with 40 μL of each compound (240 μg/disc) at the concentration of 6.0 mg mL^{-1} and placed on the inoculated agar. DMSO impregnated discs were used as negative control. Sulfamethoxazole (300 μg/disk) and sulfisoxazole (300 μg/disk) were used as positive reference standards to determine the sensitivity of one strain/isolate in each microbial species tested. The inoculated plates were incubated at 310 K for 24 h for bacterial strains isolates. Antimicrobial activity in the disc diffusion assay was evaluated by measuring the zone of inhibition against the test organisms. Each assay in this experiment was repeated twice [21].

The minimal inhibition concentration (MIC) values, except one, were also studied for the microorganisms sensitive to at least one of the five compounds determined in the disc diffusion assay. The inocula of microorganisms were prepared from 12 h broth cultures and suspensions were adjusted to 0.5 McFarland standard turbidity. The test compounds dissolved in 20% dimethylsulfoxide (DMSO) were first diluted to the highest concentration (6.0 mg mL^{-1}) to be tested, and then serial, twofold dilutions were made in a concentration range from 5.85 to 6000 μg mL^{-1} in 10 mL sterile test tubes containing nutrient broth. The MIC values of each

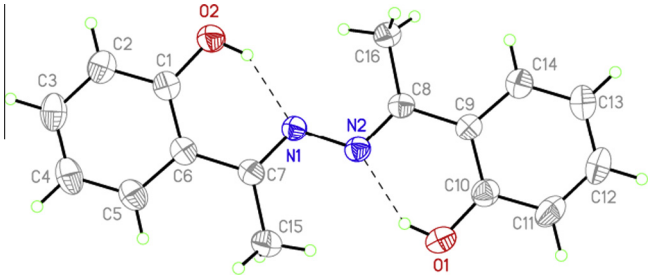

Fig. 1. View of the of 2,2′-[(1E,2E)-hydrazine-1,2-diylidenedi(1E)eth-1-yl-1-ylidene]diphenol molecule showing the atom labeling scheme and displacement ellipsoids at the 30% probability level. Hydrogen bonds are indicated by dashed lines.

compound against bacterial strains were determined based on a micro-well dilution method. The 96-well plates were prepared by dispensing 95 μL of nutrient broth and 5 μL of the inoculums into each well. One hundred μL from each of the test compounds initially prepared at the concentration of 6000 μg mL^{-1} was added into the first wells. Then, 100 μL from each of their serial dilutions was transferred into twelve consecutive wells. The last well containing 195 μL of nutrient broth without compound, and 5 μL of the inoculums on each strip, was used as negative control. The final volume in each well was 200 μL. The contents of the wells were mixed and the microplates were incubated at 310 K for 24 h. All compounds tested in this study were screened twice against each microorganism. The MIC was defined as the lowest concentration of the compounds to inhibit the growth of microorganisms [22].

Theoretical calculations

Because of the effective bioactivities of 2,2′-[(1E,2E)-hydrazine-1,2-diylidenedi(1E)eth-1-yl-1-ylidene]diphenol the three

Table 2
Selected bond distances (Å) and bond and torsion angles (°) for 2,2′-[(1E,2E)-hydrazine-1,2-diylidenedi(1E)eth-1-yl-1-ylidene]diphenol.

Bond distances (Å)			
O1—C10	1.344 (3)	C8—C9	1.470 (3)
O1—H10	0.8200	C8—C16	1.498 (3)
O2—C1	1.344 (2)	C7—C15	1.506(3)
O2—H20	0.8200	C6—C7	1.471(3)
N1—C7	1.294 (2)	N2—C8	1.297 (2)
N1—N2	1.394 (2)		
Bond angles (°)			
C10—O1—H10	109.5	C14—C9—C8	121.18 (17)
C1—O2—H20	109.5	C10—C9—C8	121.73 (19)
C7—N1—N2	116.05 (15)	O1—C10—C11	117.6 (2)
C8—N2—N1	116.09 (15)	O1—C10—C9	122.5 (2)
O2—C1—C2	117.5 (2)	C11—C10—C9	119.9 (2)
O2—C1—C6	122.23 (18)	C12—C11—C10	120.8 (2)
C9—C8—C16	119.24 (17)	N1—C7—C6	117.02 (17)
C5—C6—C7	121.53 (19)	N1—C7—C15	123.28 (19)
C1—C6—C7	121.63 (17)	C6—C7—C15	119.70 (18)
N2—C8—C9	116.64 (16)		
Torsion angles (°)			
C7—N1—N2—C8	177.78 (16)	N1—N2—C8—C9	179.43 (14)
O2—C1—C2—C3	−178.79 (19)	N1—N2—C8—C16	0.1 (3)
C16—C8—C9—C14	−1.9 (3)	N2—C8—C9—C14	178.70 (17)
C4—C5—C6—C7	179.10 (19)	N2—C8—C9—C10	−1.9 (2)
O2—C1—C6—C5	179.16 (16)	C16—C8—C9—C10	177.5 (2)
O2—C1—C6—C7	−0.3 (3)	C14—C9—C10—O1	−179.34 (19)
C2—C1—C6—C7	−179.10 (17)	C8—C9—C10—O1	1.2 (3)
N2—N1—C7—C6	179.82 (15)	C8—C9—C10—C11	−178.5 (2)
N2—N1—C7—C15	0.3 (3)	O1—C10—C11—C12	179.8 (2)
C5—C6—C7—N1	178.62 (17)	C8—C9—C14—C13	178.65 (18)
C1—C6—C7—N1	−2.0 (3)	C1—C6—C7—C15	177.6 (2)

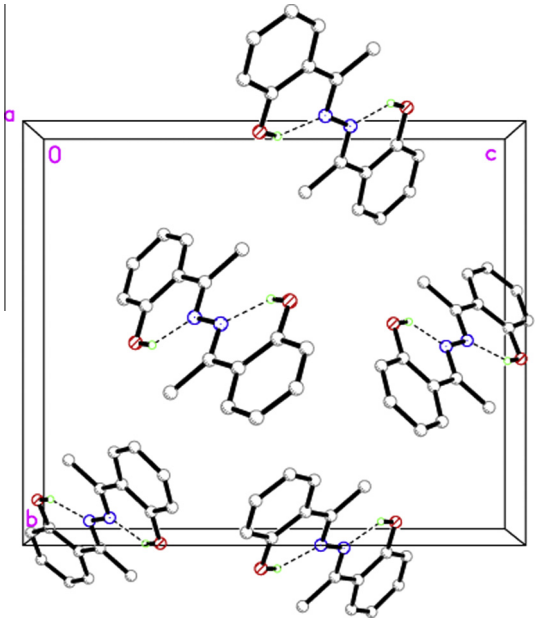

Fig. 2. The crystal packing of 2,2′-[(1E,2E)-hydrazine-1,2-diylidenedi(1E)eth-1-yl-1-ylidene]diphenol, viewed along the *a* axis.

Table 3
Hydrogen-bond geometry (Å, °) for 2,2′-[(1E,2E)-hydrazine-1,2-diylidenedi(1E)eth-1-yl-1-ylidene]diphenol.

D—H···A	D—H	H···A	D···A	D—H···A
O1—H1O···N2	0.82	1.82	2.541 (2)	147
O2—H2O···N1	0.82	1.82	2.541 (2)	146

dimensional conformation of the molecule was also determined as it will be able to give important previews about molecular behavior in gas and solution forms. In the mentioned conformational analysis, the molecular geometry optimizations and vibration frequency calculations were performed with the Gaussian 03W software package by using DFT approaches in addition to the determination of crystal structure [23]. The split valence 6-311++G(d,p) basis set was used for the expansion of the molecular orbital [24]. The geometries were fully optimized without any constraint with the help of an analytical gradient procedure implemented within the Gaussian 03W program. All the parameters were allowed to relax and all the calculations converged to an optimized geometry which corresponds to a true energy minimum as revealed by the lack of imaginary values in the wave number calculations. The ^{1}H and ^{13}C NMR chemical shifts of the compounds were calculated in $CDCl_3$ using the GIAO method. The vibrational band assignments were performed at B3LYP/6-311++G(d,p) theory level combined with scaled quantum mechanics force field (SQMFF) methodology.

Results and discussion

Molecular structure

The molecular structure 2,2′-[(1E,2E)-hydrazine-1,2-diylidenedi(1E)eth-1-yl-1-ylidene]diphenol is shown in Fig. 1, while selected bond lengths and bond and torsion angles are listed in Table 2. The molecule displays an E, E configuration with respect to the C=N double bond as seen in Fig. 1. While one of the bond lengths between the nitrogen and carbon atoms (N1—C7) conforms to the value for a double bond of 1.294(2) Å, the other (N2—C8) is closer to double bond distance value of 1.297(2) Å because of conjugation effects in the molecule. The central N1—N2 bond length of 1.394(2) Å obtained in the molecular structures of (E)-1-(2,4-Dinitrophenyl)-2-[1-(2-methoxyphenyl)ethylidene] hydrazine [25]. The structure of a hydroxyl group substituted hydrazine has been previously published by another research group [26]. The presence of hydroxyl group in the title compound has been caused more planar molecular aggregation as expected. The molecular structure indicates almost coplanar geometry. Maximum deviations can be defined by a torsion angle (C5—C6—C7—C15) of −1.8(3)° and the dihedral angle between the two benzene rings [177.8(16)°]. All the other bond lengths are within the normal ranges [27]. Unit cell arrangement (Fig. 2) viewed along clearly shows the screw axes along b and c as main geometrical and symmetrical correlations observed in space group of $P2_12_12_1$. Two intramolecular O2—H···N1 [2.541(2) Å and 2.541(2) Å] hydrogen bonds are observed. Intramolecular hydrogen bond present in the compound is given in Table 3.

The reaction of Schiff base with transition metal ions in 2:2 M ratio lead to the formation of Schiff base dinuclear complexes of the types, $[M_2L_2]$ (M = Ni(II), Pt(II), Pd(II)) (Fig. 3). The molar conductivities (Λ_m) of 10^{-3} M solutions of the complexes were measured in DMSO at room temperature. Conductivity results show that complexes are non-electrolyte. The significant electronic spectra of the ligand and complexes are recorded in DMSO. The important bands of the ligand and the complexes are observed in the region of 293–260 and 400–500 nm. The magnetic moments of the complexes (as B.M.) were measured at room temperature. The spectra of the Ni(II) complex show bands in the range of 490–498 nm, Pd(II) complex 353–354 nm and P(II) complex

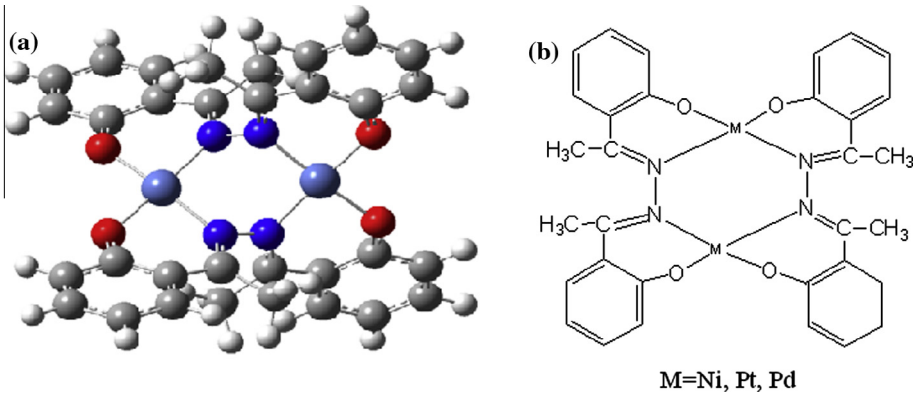

Fig. 3. (a) Optimized molecular structure of $[Ni_2L_2]$ complex and (b) suggested structure of the metal complexes.

Table 4
The comparison of the experimental and calculated values of vibrational frequencies (cm^{-1}) 2,2′-[(1E,2E)-hydrazine-1,2-diylidenedi(1E)eth-1-yl-1-ylidene]diphenol.

Assignments	Experiment	B3LYP/6-311++G(d,p) (Unscaled)	B3LYP/6-311++G(d,p) (Scaled)
υ(OH)	3439	3836	3835
$\upsilon_s(CH)_{ring}$	3060	3201	3065
$\upsilon_{as}(CH)_{ring}$	3017	3187–3145	3052–3011
$\upsilon_{as}(CH_3)$	2967	3132–3096	2999–2963
$\upsilon_s(CH_3)$	2927	3040	2910
υ(C=N)	1602	1655/1651/1632/1608	1644/1633/1612/1594
$\upsilon(CC)_{ring}$ + υ(C=N)		1651/1632/1608	1633/1612/1594
$\upsilon(CC)_{ring}$	1558	1643/1619	1622/1600
$\upsilon(CC)_{ring}$ + $\delta(CCH)_{ring}$	1493	1630–1487	1511–1449
$\delta(CH_3)$	1437	1475–1467	1437–1424
$\gamma(CH_3)$	1360	1399	1348
$\upsilon(CC)_{ring}$ + δ(COH)		1357	1340
υ(CO) + $\upsilon(CC)_{ring}$ + $\delta(CCH)_{ring}$ + δ(COH)	1295	1318	1297
$\upsilon(CC)_{ring}$ + υ(CO) + $\delta(CCH)_{ring}$	1242	1264	1249
$\upsilon(CC)_{ring}$ + $\delta(CCH)_{ring}$	1189	1182–1132	1152–1108
$\upsilon(CC)_{ring}$ + $\gamma(CH_3)$	1061	1061	1043
$\gamma(CH_3)$ (72)	1033	1050–1037	1031–1019
$\gamma(CH)_{ring}$ (80)	972	985–953	984–952
υ(N—N) (30) + $\upsilon(C—CH_3)$ (21) + υ(C=N) (7) + $\gamma(CH_3)$ (8)	940	939	926
υ(CO) (22) + $\upsilon(C—CH_3)$ (15) + δ(CCC) (24)	834	837	820
$\tau(CCCH)_{ring}$ (40)	753	756	750
δ(NNC) (17)+ δ (NC—CH_3) (11) + δ (NCC_{ring}) (9) + $\delta(CCC)_{ring}$ (8)	660	659	637
$\delta(NCC_{ring})$ (38) + δ(NNC) (14)	621	654	630
$\upsilon(CC)_{ring}$ (9) + δ(CCO) (12) + τ(NC—CH_3) (7)	563	571	556
$\delta(CCC)_{ring}$ (7) + $\tau(CCCC)_{ring}$ (6)	520	528	521
δ(CCO) (13) + $\delta(NCC_{ring})$ (9)	494	495	483
δ(CCO) (46) + τ(NNC—CH_3) (7)	456	459	446

ν: Bond stretching, δ: in-plane angle bending, γ: out-of-plane angle bending, τ: torsion, as: antisymmetric and s: symmetric.

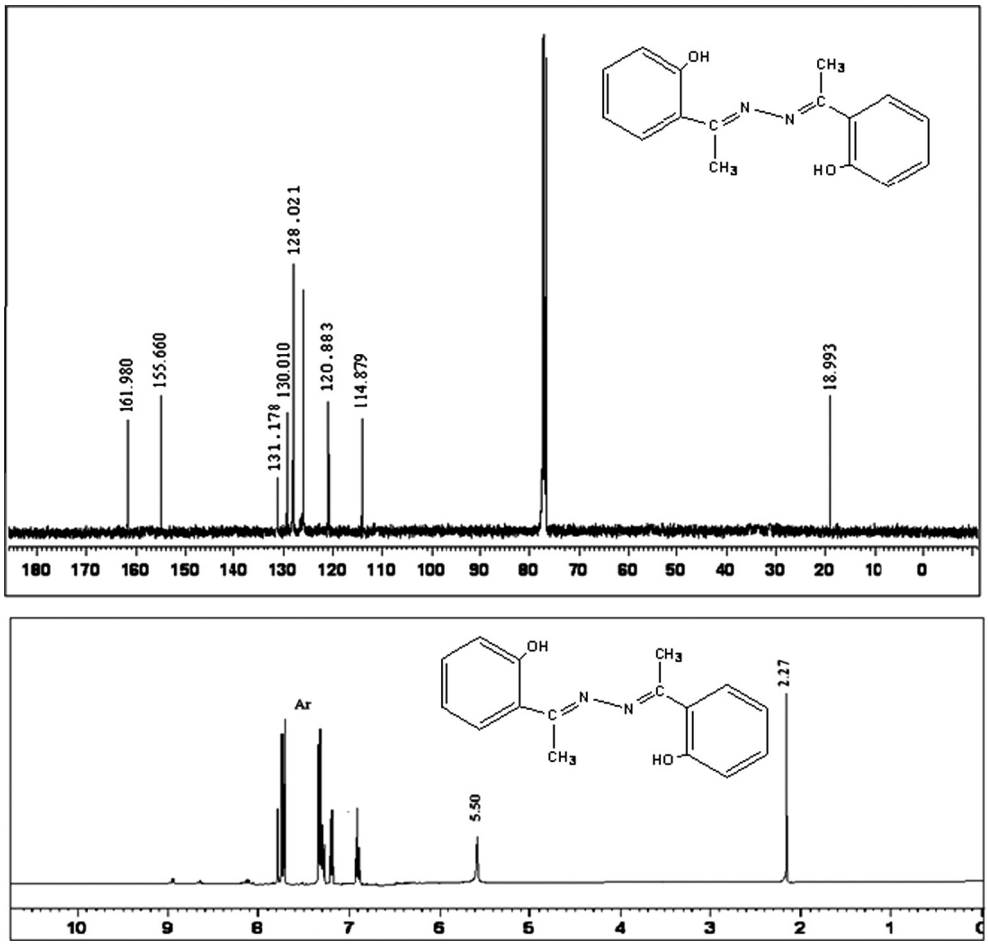

Fig. 4. The experimental ^{1}H NMR and ^{13}C NMR spectra of 2,2′-[(1E,2E)-hydrazine-1,2-diylidenedi(1E)eth-1-yl-1-ylidene]diphenol in chlorofom.

Table 5
Experimental and calculated ^{13}C NMR and ^{1}H NMR chemical shifts (ppm) for 2,2′-[(1E,2E)-hydrazine-1,2-diylidenedi(1E)eth-1-yl-1-ylidene]diphenol.

Assignment	^{1}H NMR[a]		Assignment	^{13}C NMR[*]	
	Experimental	Calculated		Experimental	Calculated
C—C**H$_3$**	2.27	2.29	**C**H$_3$	18.99	18.55
H2—H11	6.88	6.67	**C7—C8**	161.98	161.28
H3—H12	7.20	7.19	**C1—C10**	155.66	155.85
H4—H13	7.28	6.91	**C2—C11**	114.88	114.17
H5—H14	7.88	8.07	**C3—C12**	130.01	129.99
O**H**	5.50	4.38	**C4—C13**	120.88	119.79
			C5—C14	131.18	131.21
			C6—C9	128.02	128.60

[a] Calculated using GIAO/B3LYP/6-31++G(d,p) method in $CDCl_3$.

260–262 nm. Hence, square-planar structures may be assigned to these complexes [28] Also the magnetic moments of complexes (as 0.00 B.M.) were measured and therefore complexes have square-planar geometry.

FT-IR spectra

The infrared spectra of 2,2′-[(1E,2E)-hydrazine-1,2-diylidenedi(1E)eth-1-yl-1-ylidene]diphenol were recorded in the 4000∼400 cm^{-1} region using KBr pellets on a MATTSON-1000 model FT-IR spectrometer. The vibrational band assignments were performed at B3LYP/6-311++G(d,p) theory level combined with scaled quantum mechanics force field (SQMFF) methodology [29] to compare the experimental and calculated vibrational frequencies of the title compound. The visual check for the vibrational band assignments were also performed by using Gauss-View program. In order to enable assignment of the observed peaks, have analyzed the some important vibrational frequencies and compared our calculated results of the investigated compound with their experimental ones and given in Table 4.

The characteristic C—H stretching vibrations of hetero aromatic structures are expected to appear in 2900∼3150 cm^{-1} frequency ranges [30–33]. In the present study, C—H aromatic stretching modes were observed at 3060 and 3017 cm^{-1} correspond to symmetric and asymmetric stretching C—H aromatic ring modes experimentally, and calculated values of this modes were 3065 and 3052–3011 cm^{-1}. The bands at 2967 and 2927 cm^{-1} correspond to the asymmetric and symmetric stretching CH_3 group. These bands were calculated at 2999–2963 and 2910 cm^{-1}, respectively. The in-plane angle bending and out-of-plane angle bending CH_3 vibration modes computed at 1437–1424 and 1348 cm^{-1}, which observed at 1437 and 1360 cm^{-1}, respectively.

Azomethine (C═N) bond stretching vibrations were observed at 1602 cm^{-1} experimentally, while that have been calculated at 1644–1594 cm^{-1}. Another characteristic region of the Schiff bases derivative spectrum is 1100–1400 cm^{-1}, which is attributed to C— O stretching vibrations. The phenolic C—O stretching vibration was observed at 1295 cm^{-1} experimentally, while that has been calculated at 1297 cm^{-1}.

The characteristic region of the O—H group vibrations spectrum in the Schiff bases is 3550–3700 cm^{-1} [33]. In this study, the experimental O—H stretching vibration was observed at 3439 cm^{-1}. The in-plane (in phenols) angle bending vibration of the OH was observed at 1295 cm^{-1} in the FT-IR spectra. This band has been calculated at 1340 and 1297 cm^{-1}.

The calculation results of other group vibrations show good agreement with the experimental values. The important other experimental and calculated vibrational results can be seen in Table 4.

The strong bands at 1602 cm^{-1} for free ligand is due to the azomethine vibration mode, ν(C═N) shift to the lower frequencies up to 1595 cm^{-1} by the coordination through the azomethine nitrogen atoms [34,35]. Schiff base displays band at 1242 cm^{-1} belongs to phenolic C—O vibration mode, ν(C—O) respectively and this band shifts to the higher frequency in the range 1198∼1235 cm^{-1} by the coordination through the phenolic oxygen atoms in the benzene rings [36].

NMR spectra

In this study, the magnetic isotropic shielding tensors (δ_C) of the compound were calculated for the most stable conformers using GIAO /B3LYP/6-311++G(d,p) methods in chloroform ($CDCl_3$) solutions with GAUSSIAN 03 software for helping the assignment of

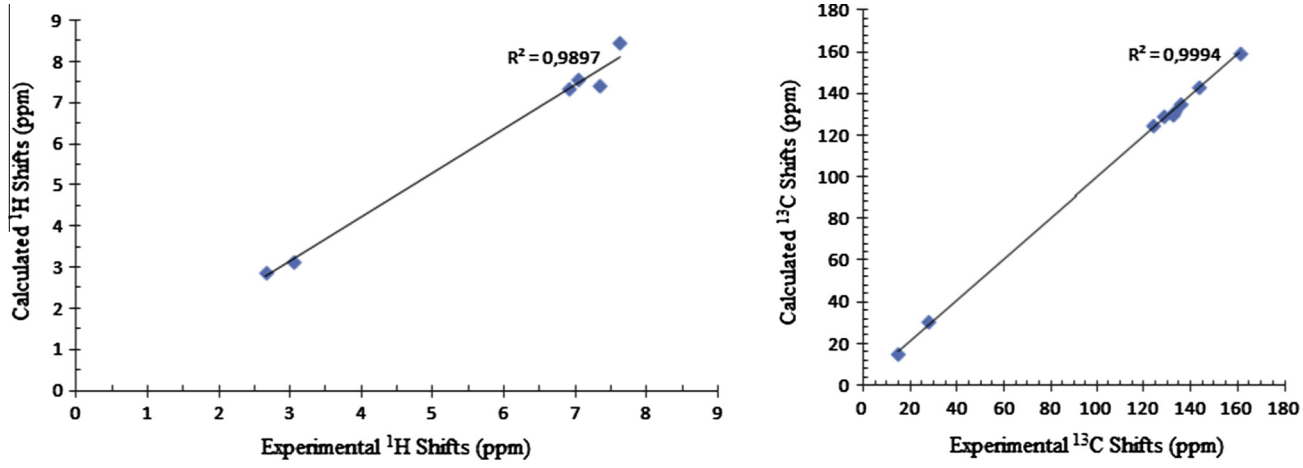

Fig. 5. Plot of the calculated vs. the experimental ^{1}H NMR and ^{13}C NMR chemical shifts of the 2,2′-[(1E,2E)-hydrazine-1,2-diylidenedi(1E)eth-1-yl-1-ylidene]diphenol.

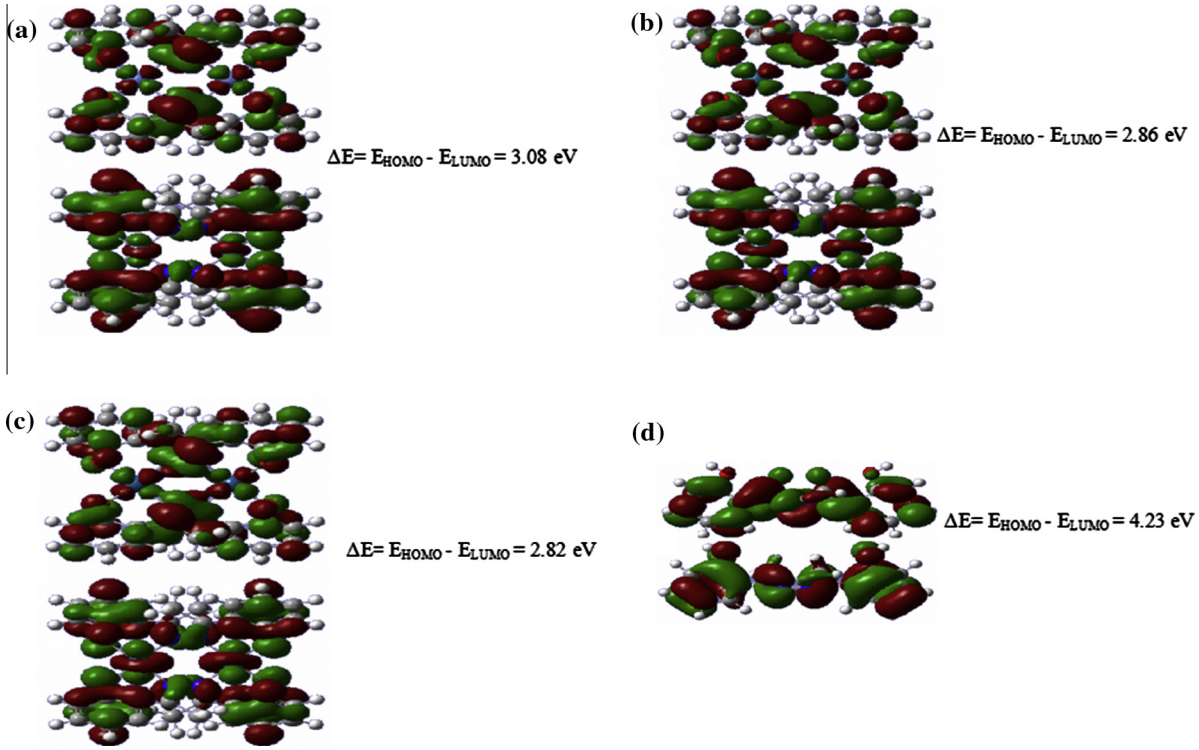

Fig. 6. (a–d) Plots of the frontier orbitals of the Ni, Pt, Pd complexes and 2,2′-[(1E,2E)-hydrazine-1,2-diylidenedi(1E)eth-1-yl-1-ylidene]diphenol molecule, respectively.

chemical shifts of carbon atoms and hydrogen atoms [23]. The ^{13}C NMR and ^{1}H NMR spectrum of the compound in chloroform are given in Fig. 4. The experimental and calculated chemical shift values are shown in Table 5. The positions of the signals of the methyl protons from C**H**$_3$C═N fragments are in agreement with the data from other Schiff bases [37]. The ^{1}H NMR spectrum of the compound, C—C**H**$_3$, proton signals gave the following results 2.27 ppm, which shows good agreement with experimental values (2.29 ppm respectively). Signals in the δ 6.89–7.88 ppm region belong to aromatic Ar—**H**-atoms. Absorptions at δ 18.99 ppm were assigned to their C—**C**H$_3$ atoms (calculated 18.55 ppm respectively). Signals in the δ 114.06–155.85 ppm region belong to aromatic Ar—**C**-atoms. The ^{13}C NMR spectrum of the compound, **C**—CH$_3$, carbon signals gave the following results 161.28 ppm, which shows good agreement with experimental values (161.98 ppm respectively). According to these results, the calculated chemical shifts are in compliance with the experimental findings. The correlation graphic based on the calculated values and experimental data of the compound data has also been given in Fig. 5. The correlation values for proton and carbon chemical shifts are found to be 0.9897, 0.9994 for B3LYP with the 6-311++G(d,p) basis set.

Frontier molecular orbital analysis

The calculations indicate that the ligand and complex compounds have 71 and 158 occupied molecular orbital, respectively. The energy gap for mentioned compounds between the highest occupied molecular orbital (HOMO) and the lowest unoccupied molecular orbital (LUMO) energies, have been calculated and is

Table 6
The MICs of antibacterial activity (concentration used 6.0 mg/mL of 20% DMSO) of 2,2′-[(1E,2E)-hydrazine-1,2-diylidenedi(1E)eth-1-yl-1-ylidene]diphenol and its complexes.

Bacteria strains	Newly synthesized compounds (μg/mL/(mM))					
Gram-negative	L	$Ni2L_2$	Pt_2L_2	Pd_2L_2	SD1	SD2
Escherichia coli ATCC 11230	375	187.5	93.75	93.75	64	23.5
	(1.39)	**(0.28)**	**(0.10)**	**(0.125)**	**(0.25)**	**(0.088)**
Pseudomonas aeruginosa ATCC 15442	93.7	46.87	46.87	23.43	64	375
	(0.35)	**(0.071)**	**(0.05)**	**(0.031)**	**(0.25)**	**(1.40)**
Klebsiella pneumoniae ATCC 70063	187.5	93.75	46.87	46.87	16	23.5
	(0.70)	**(0.14)**	**(0.05)**	**(0.062)**	**(0.063)**	**(0.068)**
Gram-positive						
Bacillus subtilis ATCC 6633	375	187.5	93.75	93.75	1500	–
	(1.39)	**(0.28)**	**(0.10)**	(0.125)	**(5.92)**	
Bacillus cereus NRRL-B-3711	750	375	187.5	93.75	16	375
	(2.80)	**(0.57)**	**(0.20)**	**(0.125)**	**(0.063)**	**(1.40)**
Staphylococcus aureus ATCC 6538	750	375	187.5	46.87	32	93.75
	(2.80)	**(0.57)**	**(0.20)**	**(0.062)**	**(0.126)**	**(0.35)**
Enterococcus faecalis ATCC 29212	1500	187.5	93.75	46.87	32	93.75
	(5.60)	**(0.28)**	**(0.10)**	**(0.062)**	**(0.126)**	**(0.35)**
Streptococcus agalactiae ATCC 13813	187.5	93.375	46.87	46.87	16	11.8
	(0.70)	(0.14)	(0.05)	**(0.062)**	**(0.063)**	**(0.044)**

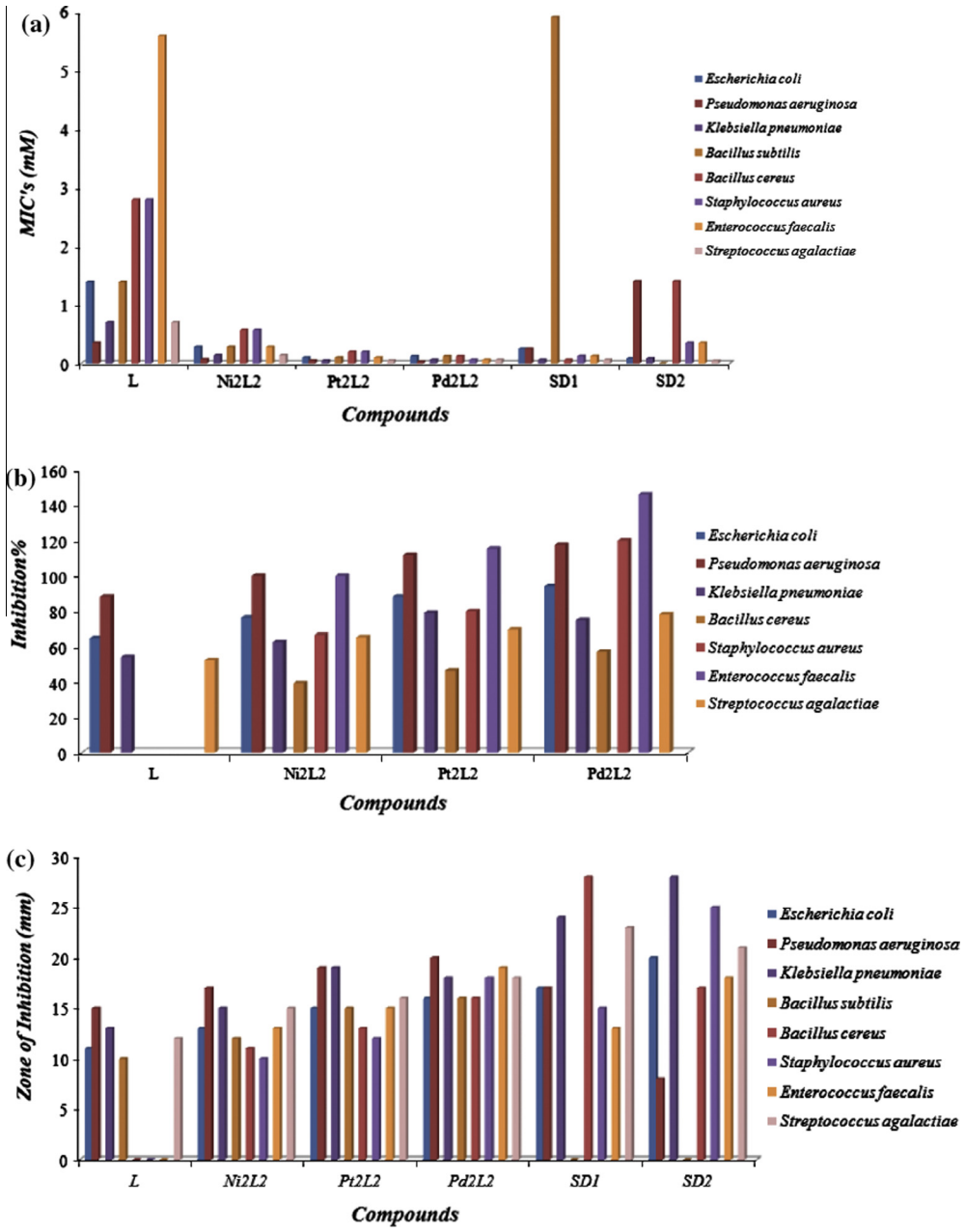

Fig. 7. (a) Comparison of antibacterial activite (MIC) of compounds; (b) comparison of antibacterial activite (disc) of compounds and (c) percentage of inhibition for the compounds.

given in Fig. 6. The frontier molecular orbitals play an important role in the electronic and optical properties, as well as in UV–vis spectra and chemical reactions [38]. Also, the energy gap between HOMO and LUMO is a critical parameter in determining molecular electrical transport properties and electronic systems with a larger HOMO–LUMO gap should be less reactive than those with a smaller gap [39]. The energy gap of HOMO–LUMO explains the prospective charge transfer interaction within the molecule, and in this study, the frontier orbital energy gap in case of ligand compound is found to be 4.23 eV obtained at B3LYP method using LanL2DZ basis set. Also, the frontier orbital energy gap for Ni, Pt and Pd complex was found to be 3.08, 2.82, and 2.86 eV obtained at B3LYP method using LanL2DZ basis set, respectively. According to these results, band gap of the complex compounds decreases to about 30–38%.

The LUMO energy is most important descriptors which describe electrophilicity of the compound and its level has the importance because of the donor–acceptor interactions. Generally, molecules with lower LUMO energy values accept the electrons more easily than higher's. The lower LUMO energy and larger $\Delta E_{(\text{HOMO-LUMO})}$ gap affect the binding affinities to the biologic molecules, therefore LUMO energy and $\Delta E_{(\text{HOMO-LUMO})}$ gap are important factors for activities of hydrazine compounds .

The biological activity is reverse relationship to the $\Delta E_{(\text{HOMO-LUMO})}$ gap. The biological activity of the studied compounds increases with the lower $\Delta E_{(\text{HOMO-LUMO})}$ gap. Respective values of $\Delta E_{(\text{HOMO-LUMO})}$ band gap and biologic activity are in following orders. For $\Delta E_{(\text{HOMO-LUMO})}$ gap: ligand molecule < Ni complex < Pt complex < Pd complex and for biological activity: ligand molecule < Ni complex < Pt complex < Pd complex.

Table 7
Measured inhibition zone diameter (mm) of the, 2,2′-(1E,1′E)-1,1′-(hydrazine-1,2-diylidene)bis(ethan-1-yl-1-yliden)diphenol and its complexes.

Bacteria strains	Diameter inhibition zone (mm, 240 μg/disk)					
	L	Ni_2L_2	Pt_2L_2	Pd_2L_2	SD1	SD2
Gram-negative						
Escherichia coli ATCC 11230	11	13	15	16	17	20
Pseudomonas aeruginosa ATCC 15442	15	17	19	20	17	8
Klebsiella pneumoniae ATCC 70063	13	15	19	18	24	28
Gram-positive						
Bacillus subtilis ATCC 6633	10	12	15	16	–	–
Bacillus cereus NRRL-B-3711	–	11	13	16	28	17
Staphylococcus aureus ATCC 6538	–	10	12	18	15	25
Enterococcus faecalis ATCC 29212	–	13	15	19	13	18
Streptococcus agalactiae ATCC 13813	12	15	16	18	23	21

SD_1: sulfamethoxazole (300 μg/disk), SD_2: sulfisoxazole (300 μg/disk) <10: weak; >10 moderate; >16: significant.

In vitro antibacterial activity

2,2′-[(1E,2E)-hydrazine-1,2-diylidenedi(1E)eth-1-yl-1-ylidene]-diphenol and metal(II) complexes were screened in vitro for its antibacterial activity against five Gram-positive species (*Bacillus subtilis*, *Bacillus cereus*, *Staphylococcus aureus*, *Enterococcus faecalis* and *Streptococcus agalactiae* and three Gram-negative species (*Escherichia coli*, *Pseudomonas aeruginosa* and *Klebsiella pneumoniae*)) by the microdilution (Table 6, Fig. 7a) and disc diffusion methods (Table 7, Fig. 7b). The results were compared with those of the standard drugs sulfamethoxazole and sulfioxazole (Fig. 7a–c).

As the disc diffusion assay results evidently show (Table 7, Fig. 7b) that *Pt_2L_2 and Pd_2L_2* has exhibited the strong inhibition effect against most of test bacteria whereas ligand has weaker activity. Similar results were also reported by Jin et al. [40].

The complexes show the highest activities against *P. aeruginosa* which is the mostly effected by *Pd_2* L_2 having the diameter zone of 20 mm. All compounds except ligand have significant activity against *P. aeruginosa* at in the diameter zone of 17–20 mm whereas sulfisoxazole, the drug used as standard, has been found less active (8 mm) against the bacteria mentioned above.

Percentage of inhibition for the compounds exhibited in Fig. 7c that *Pd_2L_2* shows excellent activity while other metal complexes have good activity or moderate activity against *P. aeruginosa*.

According to the MIC's results shown in Table 6 the compounds possess a broad spectrum of activity against the tested bacteria at the concentrations of 23.46–1500 μg/mL. The *Pd_2L_2 and Pt_2L_2* have shown activity against *B. cereus* NRRL-B-3711 at a concentration of 187.5 μg/mL (0.2 mM), 93.75 μg/mL (0.125 mM) whereas sulfisoxazole, the drug used as standard, has been found less active against the bacteria.

Conclusion

2,2′-(1E,1′E)-1,1′-(hydrazine-1,2-diylidene)bis(ethan-1-yl-1-yliden) diphenol and its dimeric, binuclear Ni(II), Pd(II) and Pt(II) metal complexes were synthesized. Hydrazine and its complexes were characterized by elemental analyses, LC-MS, IR, electronic spectra, ^1H and ^{13}C NMR spectra, conductivity, magnetic measurements quantum chemical methods.

The antibacterial activities of all of the compounds are determined against Gram-positive bacteria (*Bacillus subtilis* ATCC 6633, *Bacillus cereus* NRRL-B-3711, *Staphylococcus aureus* ATCC 6538, *Enterococcus faecalis* ATCC 29212, *Streptococcus agalactiae* ATCC 13813 and three Gram-negative bacteria (*Escherichia coli* ATCC 11230, *Pseudomonas aeruginosa* ATCC 15442, *Klebsiella pneumoniae* ATCC 70063) by both disc diffusion and microdilution methods. The highest activity values are measured for the Pd(II) complexes against *P. aeruginosa*.

Acknowledgments

The authors would like to thank Ahi Evran University BAP (Grant No: FBA-11-30) for the financial support of this project. R.J.B. acknowledges the NSF-MRI program (Grant No. CHE-0619278) for funds to purchase the diffractometer.

Appendix A. Supplementary material

Supplementary data associated with this article can be found, in the online version, at http://dx.doi.org/10.1016/j.saa.2014.03.034.

References

[1] S. Rollas, S.G. Küçükgüzel, Molecules 12 (2007) 1910–1939.
[2] K. Yamada, K. Yasuda, N. Fujiwara, Z. Siroma, H. Tanaka, Y. Miyazaki, T. Kobayashi, Electrochem. Commun. 5 (2003) 892–896.
[3] S. Amlathe, V.K. Gupta, Analyst 113 (1988) 1481–1483.
[4] S.M. Golabi, H.R. Zara, J. Elecroanal. Chem. 465 (1999) 168–176.
[5] A. Poso, A.V. Wright, J. Gynther, Mutat. Res. 332 (1995) 63–71.
[6] G. Choudhary, H. Hansen, Chemosphere 37 (1998) 801–843.
[7] K.M. Korfhage, K. Ravichandran, R.P. Baldwin, Anal. Chem. 56 (1984) 1514–1517.
[8] S.G. Küçükgüzel, E.E. Oruç, S. Rollas, F. Şahin, A. Özbek, Eur. J. Med. Chem. 37 (2002) 197–206.
[9] Y. Jin, A.G. Zhong, C.H. Ge, F.Y. Pan, J.G. Yang, Y. Wan, M. Xie, H.W. Feng, J. Mol. Struct. 1010 (2012) 190–196.
[10] V.S. Palekar, A.J. Damle, S.R. Shukla, Eur. J. Med. Chem. 44 (2009) 5112–5116.
[11] M.V. Angelusiu, S.F. Barbuceanu, C. Draghici, G.L. Almajan, Eur. J. Med. Chem. 45 (2010) 2055–2062.
[12] L.D.S. Yadav, S. Sing, Indian J. Chem. 40B (2001) 440–442.
[13] (a) D. Sutton, Chem. Rev. 93 (1993) 995–1022;
(b) H. Kisch, P. Holzmeier, Adv. Organomet. Chem. 34 (1992) 67–109;
(c) H. Zollinger, Diazo Chemistry II, V.C.H. Weinheim, Germany, 1995;
(d) B.F.G. Johnson, B.L. Haymore, J.R. Dilworth, in: G. Wilkinson, R.D. Gillard, J.A. McCleverty (Eds.), Comprehensive Coordination Chemistry, vol. 2, Pergamon Press, Oxford, UK, 1987.
[14] (a) J.L. Crossland, L.N. Zakharov, D.R. Tyler, Inorg. Chem. 46 (2007) 10476–10478;
(b) S. Dabb, B. Messerle, G. Otting, et al., Chem. Eur. J. 14 (2008) 10058–10065;
(c) L.D. Field, H.L. Li, A.M. Magill, Inorg. Chem. 48 (2009) 5–9;
(d) L.D. Field, H.L. Li, S.J. Dalgarno, Inorg. Chem. 49 (2010) 6211–6214.
[15] G. Albertin, S. Antoniutti, A. Bacchi, M. Boato, G. Pelizz, J. Chem. Soc. Dalton Trans. 17 (2002) 3313–3320.
[16] M.D. Fryzuk, S.A. Johnson, Coord. Chem. Rev. 379 (2000) 200–202.
[17] S. Gupta Sreerama, S. Pal, Inorg. Chem. 44 (2005) 6299–6307.
[18] B.A. El-Sayed, M.M. Abo Aly, A.A.A. Emara, S.M.E. Khalil, Vibr. Spectrosc. 30 (2002) 93–100.
[19] CrysAlisPro 2010. Agilent Technologies, Version 1.171.35.15 (release 03-08-2011 CrysAlis171.NET) Oxford Diffraction CrysAlis PRO. Oxford Diffraction Ltd Yarnton, England.
[20] G.M.A. Sheldrick, Short history of SHELX, Acta Cryst. A64 (2008) 112–122.
[21] A.W. Bauer, W.M. Kirby, J.C. Sherris, M. Turck, Am. J. Clin. Pathol. 45 (1966) 493–496.
[22] S.G. Küçükgüzel, A. Mazi, F. Sahin, S. Öztürk, J. Stables, Eur. J. Med. Chem. 38 (2003) 1005–1013.
[23] M.J. Frisch, G.W. Trucks, H.B. Schlegel, G.E. Scuseria, M.A. Robb, J.R. Cheeseman, J.A. Montgomery Jr., T. Vreven, K.N. Kudin, J.C. Burant, J.M. Millam, S.S. Iyengar, J. Tomasi, V. Barone, B. Mennucci, M. Cossi, G. Scalmani, N. Rega, G.A. Petersson, H. Nakatsuji, M. Hada, M. Ehara, K. Toyota, R. Fukuda, J. Hasegawa,

M. Ishida, T. Nakajima, Y. Honda, O. Kitao, H. Nakai, M. Klene, X. Li, J.E. Knox, H.P. Hratchian, J.B. Cross, C. Adamo, J. Jaramillo, R. Gomperts, R.E. Stratmann, O. Yazyev, A.J. Austin, R. Cammi, C. Pomelli, J.W. Ochterski, P.Y. Ayala, K. Morokuma, G.A. Voth, P. Salvador, J.J. Dannenberg, V.G. Zakrzewski, S. Dapprich, A.D. Daniels, M.C. Strain, O. Farkas, D.K. Malick, A.D. Rabuck, K. Raghavachari, J.B. Foresman, J.V. Ortiz, Q. Cui, A.G. Baboul, S. Clifford, J. Cioslowski, B.B. Stefanov, G. Liu, A. Liashenko, P. Piskorz, I. Komaromi, R.L. Martin, D.J. Fox, T. Keith, M.A. Al-Laham, C.Y. Peng, A. Nanayakkara, M. Challacombe, P.M.W. Gill, B. Johnson, W. Chen, M.W. Wong, C. Gonzalez, J.A. Pople, Gaussian 03: Revision B.04, Gaussian, Inc., Pittsburgh, PA, 2003.
[24] P.C. Hariharan, J.A. Pople, J. Chem. Phys. 27 (1974) 209–214.
[25] H.K. Fun, B. Nilwanna, P. Jansrisewangwong, T. Kobkeatthawin, S. Chantrapromma, Acta Cryst. E67 (2011) 3202–3203.
[26] S. Chantrapromma, P. Jansrisewangwong, H.K. Fun, Acta Cryst. E66 (2010) 2994–2995.
[27] F.H. Allen, O. Kennard, D.G. Watson, L. Brammer, A.G. Orpen, R. Taylor, J. Chem. Soc. Perkin Trans. II (1987) 1–12.
[28] A.B.P. Lever, Inorg. Elect. Spect., 2nd ed., Elsevier, Amsterdam, 1984.
[29] G. Fogarasi, P. Pulay, Ab initio calculation of force fields and vibrational spectra, Vibrational Spectra and Structure a Series: of Advances, vol. 14, Elsevier, Amsterdam, 1985 (Chapter 3).
[30] R.M. Silverstein, G.C. Bassler, T.C. Morrill, Spectrometric Identification of Organic Compounds, Wiley, New York, 1981.
[31] V. Krishnakumar, R. Ramasamy, Spectrochim. Acta A 62 (2005) 570–577.
[32] G. Varsanyi, Assignments of vibrational spectra of 700 Benzene derivatives, Wiley, New York, 1974.
[33] A. Teimouri, A.N. Chermahini, K. Taban, H.A. Dabbagh, Spectrochim. Acta A 72 (2009) 369–377.
[34] G.G. Mohamed, Spectrochim. Acta A 64 (2006) 188–195.
[35] A.M. Donia, H.A. El-Boraey, Trans. Met. Chem. 18 (1993) 315–318.
[36] A.L. Vance, N.W. Alcock, J.A. Heppert, D.H. Busch, Inorg. Chem. 37 (1998) 6912–6920.
[37] Ü. Özdemir, P. Güvenç, E. Şahin, F. Hamurcu, Inorg. Chim. Acta 362 (2009) 2613–2618.
[38] Ç. Yüksektepe, H. Saraçoğlu, N. Çalışkan, İ. Yılmaz, A. Çukurovalı, Bull. Korean Chem. Soc. 31 (2010) 3553–3560.
[39] V. Arjunan, P.S. Balamourougane, et al., J. Mol. Struct. 1003 (2011) 92–102.
[40] Y.X. Jin, A.G. Zhong, C.H. Ge, F.Y. Pan, J.G. Yang, Y. Wu, M. Xie, H.W. Feng, J. Mol. Struct. 1010 (2012) 190–196.